A crevice adjoining the ribosome tunnel: Hints for cotranslational folding

Maya Amit[a,1], Rita Berisio[b,1], David Baram[a], Joerg Harms[c,2], Anat Bashan[a], Ada Yonath[a,*]

[a] *Department of Structural Biology, The Weizmann Institute, 76100 Rehovot, Israel*
[b] *Institute of Biostructure and Bioimaging, CNR, 80138 Napoli, Italy*
[c] *Max-Planck Research Unit for ribosomal Structure, Hamburg 22603, Germany*

Accepted 15 March 2005

Available online 23 March 2005

Edited by Horst Feldmann

Abstract RNA protection experiments and the crystal structure of a complex of the large ribosomal subunit from the eubacterium *Deinococcus radiodurans* with rapamycin, a polyketide compound resembling macrolides and ketolides, showed that rapamycin binds to a crevice located at the boundaries of the nascent protein exit tunnel, near its entrance. At this location rapamycin cannot occlude the ribosome exit tunnel, consistent with its failure to act as a ribosomal antibiotic drug. In accord with recent biochemical data, this crevice may play a role in facilitating local cotranslational folding of nascent chains, in particular for transmembrane proteins.

Keywords: Ribosome; Rapamycin; Tunnel crevice; Nascent chain; Cotranslational folding; Macrolide binding pocket

1. Introduction

Nascent proteins emerge out of the ribosome through an exit tunnel, a universal feature of the large ribosomal subunit. The entrance to this tunnel is adjacent to the peptidyl transferase center (PTC), and its opening is located at the other end of the subunit. High-resolution crystal structures showed that the tunnel is rather kinked, has a non-uniform diameter, and contains grooves and cavities [1,2]. Originally, this tunnel was assumed to be a firmly built passive path [1] that does not interact with the nascent proteins and is not involved in their progression. However, biochemical results, accumulated during last decade, indicate that the tunnel plays an active role in sequence-specific gating of nascent chains (reviewed in [3–8]) and in responding to cellular signals. Indeed, crystal structures of complexes of the large ribosomal subunit from the eubacterium *Deinococcus radiodurans* indicated that the tunnel has the capability to oscillate between conformations, and that these alterations could be correlated with nascent protein sequence discrimination and gating [9], as well as with its trafficking into its chaperone-folding cradle [10].

At its entrance the tunnel diameter may limit the passage of folded polypeptides. Furthermore, in specific cases, likely be connected with nascent-chain-tunnel interactions, it may hamper the progression of protein sequences known to arrest elongation [11,12]. The rotatory motion that translocates the aminoacylated A-site tRNA 3′ end into the P-site while peptide bond is being formed [13] dictates that the side chains of successive residues are pointing to opposite sides. Hence,nascent proteins enter into the tunnel at an extended conformation, which complies well with the tunnel narrow entrance as well as with the suggestion that motions of rigid residues, such as prolines, may be restricted under specific cellular conditions [10,14].

So far most of the tunnel functional roles have been attributed to mobile extended loops of ribosomal proteins that penetrate its walls, which are primarily made of ribosomal RNA. Examples are the tips of extended loops of proteins L22 and L23. Thus, the beta-hairpin tip of L22 that can swing across the tunnel around its accurately placed hinge, appears to provide the mechanism for elongation arrest when triggered by specific cellular conditions [9,15]. Similarly, the tip of L23 internal loop undergoes allosteric conformational changes that can modulate the shape and the size of the tunnel opening upon binding the trigger factor, the first chaperone encountering the emerging nascent chain in eubacteria [10]. Both can provide communication routes for signaling between the ribosome and the cell, as their other ends are located on the solvent side of the ribosome, in the proximity of the tunnel opening [9,15].

The protein exit tunnel is the target of macrolide antibiotics, which rank highest in clinical usage and act by producing a steric blockage of the ribosome exit tunnel, hence hampering the progression of nascent chains [9,16–19]. These natural and semi-synthetic compounds are characterized by a macrolactone ring to which at least one sugar moiety is attached (Fig. 1). Ketolides belong to a novel class of the macrolide family, characterized by a keto group at position 3 of the macrolactone ring, a single amino-sugar moiety and an extended hydrophobic arm. This recently developed drug family was designed to act against several macrolide resistant bacterial strains. High-resolution crystal structures of complexes of macrolides and ketolides with D50S [16–18], an excellent pathogen model for these studies, showed that they bind to a specific pocket in the eubacterial tunnel, called below the macrolide binding-pocket. These crystallographically observed macrolide interactions illuminated resistance mechanisms involving rRNA modification. Alterations in the tunnel conformation seen crystallographically [9], and the structural analysis of the nature of the dynamic tunnel constriction, built of the tips of extended loops of L22 and L4 [20], could be correlated with

*Corresponding author.
E-mail address: ada.yonath@weizmann.ac.il (A. Yonath).

[1] These authors contributed equal to this work.
[2] riboworld.com.

0014-5793/$30.00
doi:10.1016/j.febslet.2005.03.023

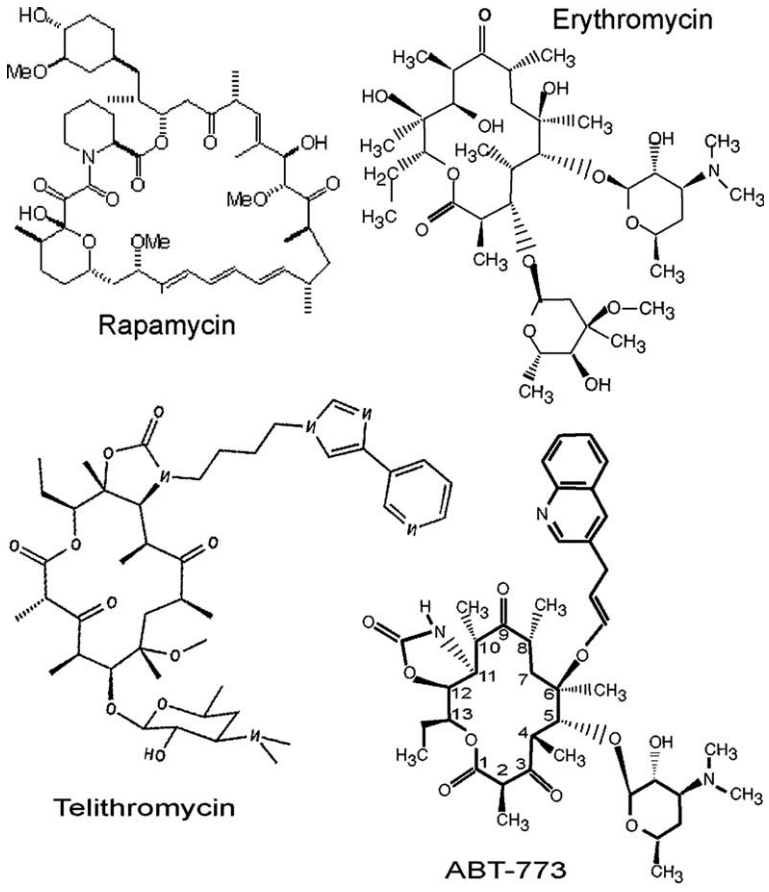

Fig. 1. Chemical structures of rapamycin, erythromycin, telithromycin and ABT-773.

the antibiotic-resistant mechanisms involving ribosomal proteins [10,21–23].

Rapamycin, a compound isolated from a strain of *Streptomyces hygroscopicus,* resembles to some extent, the molecular structures of antibiotics from the macrolide/ ketolide family, sharing with them a rather hydrophobic lipophilic ring, but lacking the sugar moieties [24,25] (Fig. 1). This polyketide serves as an immunosuppressive agent and has a strong impact on the control of biosynthesis in both unicellular and multi-cellular eukaryotes. Once bound to its receptor, the immunophilin FKBP, rapamycin targets the evolutionarily conserved TOR (target of rapamycin) proteins, which are effectors for signals indicating to the cell whether the external conditions are adequate for growth in both unicellular and multi-cellular organisms [26]. It was also shown that TOR controls 35S and 5S rRNA synthesis via RNA polymerase I and polymerase III, respectively [27,28], and ribosomal proteins gene expression via the transcription factor FHL1 [29]. Rapamycin treatment mimics nutrient deprivation. Consequently, ribosome production is curtailed through TOR functions, or a cell may even begin to degrade ribosomes, in a process called autophagy. In addition, rapamycin causes substantial changes in the cellular transcriptome and reduces protein synthesis by targeting the initiation step of translation [30]. A similar signaling mechanism does not exist in bacteria, where biosynthesis is directly controlled by aminoacid and ATP abundance [31,32].

Given its structure similarity to macrolides, we assumed that rapamycin might bind to the tunnel of eubacterial ribosomes and shed light on the tunnel binding capabilities, although is not known as a powerful ribosomal antibiotic. We therefore conducted crystallographic analysis of rapamycin complexed with the large ribosomal subunit of *D. radiodurans* (D50S) and verified our results by RNA probing. Here, we show that rapamycin binds to a crevice, built exclusively of 23S RNA nucleotides, located at the tunnel wall opposite to the macrolide-binding site. These findings confirm that the tunnel possesses specific binding properties. We suggest that the identified binding crevice in the tunnel plays a role in nascent protein progression, despite the initial description of the tunnel as a "non-sticky" path [1].

2. Materials and methods

2.1. Base numbering

Nucleotides are numbered according to *Escherichia coli* numbering, unless specified by DR for *D. radiodurans.*

2.2. Crystallization, data collection and processing

Co-crystals of D50S with 0.01 mM rapamycin were grown using the hanging drop method, as in [2]. Data were collected at 90–100 K at ID29/ESRF/EMBL and ID19/APS/ANL, and recorded on Quantum-210 and APS detectors, respectively. Data were processed and scaled with the DENZO/SCALEPACK/HKL2000 package [33] and their statistics are shown in Table 1.

2.3. Rapamycin placement and structure refinement

Overall and group rigid body refinements were performed with CNS [34] using the 3.0 Å resolution structure of D50S as a starting model [2]. SigmaA-weighted ($F_o - F_c$) and ($2F_o - F_c$) maps indicated signifi-

Table 1
Crystallographic data

Space group	*I*222
Wavelength (Å)	0.939
Unit cell parameters (Å)	168.5, 404.0, 689.0
Resolution range (Å)	20-3.8
Mosaicity (°)	0.3
Number of unique reflections	191 012
Completeness (%)	82.8 (75.0)
*R*merge (%)	16 (56)
$\langle I\rangle/\langle\sigma(I)\rangle$	6.1 (1.6)
Redundancy	2.1
R-factor/*R*-free (%)	27.3/36.8 (5%)
r.m.s. deviations from ideality	
Bond lengths (Å)	0.003
Bond angles (°)	0.61

Values in parentheses refer to the highest resolution shell (Å).

cant difference electron density for rapamycin. The conformations of rapamycin and of the nucleotides involved in its binding were modeled interactively using the graphics model building program O [35]. Positional and residue temperature factors refinements of the obtained model were alternated with rounds of model building. The free-R factor, computed using 5% of the data, was used to monitor the refinement (Table 1). The structure exhibits good stereochemistry, as analyzed by Procheck [36]. Modeling of a nascent chain in the exit tunnel was carried out with O [35]. The percentage of accessible surface (AS) upon binding was calculated, using the CCP4 package [36], as the difference between the AS of an isolated rapamycin and that of a bound one, divided by the AS of an isolated rapamycin. Coordinates have been deposited in the protein data bank (accession code 1Z58). The structural figures were produced with RIBBONS [37].

2.4. RNA probing by footprinting experiments

(a) Antibiotic binding to ribosomal particles. One A_{260} unit (36 pmol) of D50S subunit of the ribosome was incubated at 37 °C for 30 min with rapamycin (Sigma) at concentrations ranging from 1 to 100 μM in a buffer containing 10 mM HEPES, 10 mM $MgCl_2$, and 60 mM NH_4Cl, in sterile microcentrifuge tubes.

(b) Footprinting. Following antibiotic binding, the ribosomes were incubated at 42 °C for 10 min and on ice for additional 10 min, in DMS modification buffer. The DMS modification was carried out on ice, essentially as described in [38]. Primer extension was preformed using several DNA primers designed to complement 23S rRNA regions located at the vicinity of the crystallographically determined macrolide binding pocket and rapamycin binding region, including GCCGATATGGACTC, aimed at modifications of for A2418DR (2439EC) and C2419DR (2440EC).

3. Results and discussion

3.1. Rapamycin binding site

The crystal structure of D50S co-crystallized with rapamycin shows clearly (Fig. 2A) that rapamycin binds to a crevice located at the tunnel wall, in the vicinity of the macrolide-binding pocket and the dynamic tunnel-constriction, and that rapamycin interacts with RNA nucleotides of domains V, II and IV (Fig. 2B). It also indicates that rapamycin interacts solely with the 23S RNA (Fig. 2C) via hydrophobic interactions and hydrogen bonds, and about 60% of its surface area is buried upon binding. The crystallographically determined binding site was verified by chemical RNA probing.

Rapamycin binding crevice is located closer to the PTC than the macrolide-binding pocket. The locations of the centers of mass of erythromycin and rapamycin in the ribosome tunnel are separated by about 11 Å away from each other. Hence, nascent proteins, progressing through the tunnel, will pass near the rapamycin-binding crevice before reaching the macrolide-binding pocket and the dynamic tunnel constriction (Fig. 3A and B). Importantly, rapamycin-binding fashion is dramatically different from that of macrolides and ketolides (Figs. 2C and 3B and C). Nevertheless, some of rapamycin interactions with domain V, such as those with nucleotides C2586, A2587 and U2609, are typical of macrolides, whereas no contacts are observed with 2058, the 23S RNA nucleotide that provides the primary macrolide binding interactions and is involved in macrolide selectivity and resistance (for review see [40]). In accord with the rapamycin crystallographic positioning, rapamycin binding significantly modifies the accessibility of nucleotides C2440 (C2419DR) and A2439 (A2418DR) to chemical probing (Fig. 2), indicating that these two nucleotides are protected by rapamycin. The major decrease in accessibility (~75%) was observed for C2440 (C2419DR), consistent with the proximity (~4 Å) of its ribose O2′ to the O3 of rapamycin. Even A2439 (A2418DR), which is not directly involved in rapamycin binding, but is partially masked by rapamycin, showed about 40% decrease in accessibility to DMS.

On the other hand, rapamycin-binding site partially overlaps with the location of the far end of the ketolides telithromycin [16] and ABT-773 [17] (Fig. 3C). In particular, drug interactions involving the nucleotide U790 (C803DR), belonging to helix H35 of domain II of the 23S RNA (Fig. 2B), were observed also for the extended arms of telithromycin [16] and ABT-773 (Fig. 1) [17]. Similarly, contacts with the domain IV nucleotide U1782 (C1773DR) (Fig. 2B) have been suggested to stabilize ABT-773 binding [17].

Altogether, these findings indicate that the crevice formed by domain II nucleotides U790 (C803DR) and A752 (C765DR) and domain IV nucleotides C1781 and U1782 (C1772DR and C1773DR) has a high potential for the binding of rapamycin-like compounds. Therefore, this crevice provides an alternative anchoring point for compounds that cannot interact with the nucleotide at position 2058 (2041DR) because of resistance-induced modifications or the absence of a desosamine sugar. This is consistent with the proposal that the interactions with such binding crevice provide additional binding capabilities to ketolides, even when A2058 (A2041DR) is methylated or mutated [16,17,41].

3.2. Functional implications

The existence of a crevice that has the ability to provide a specific binding site suggests that it may play a role in ribosome function. This crevice is of a size suitable for accommodating small secondary structural elements, and therefore may provide the newly born protein with a site for adopting a particular fold at the early stage of tunnel passage. This is consistent with a large range of biochemical evidence, obtained mainly for transmembrane proteins, implicating cotranslational folding [3–8]. Transmembrane segments are, similar to rapamycin, highly hydrophobic, and therefore may be accommodated within the crevice. Hence, the identified crevice may provide the space as well as a proper hydrophobic patch that might act as an inner-tunnel chaperone, consistent with findings interpreted as nascent chain folding near the PTC, which was proposed to correlate with sequential closing and opening of the translocon at the ER membrane [42].

Cotranslational folding is frequently observed for eukaryotic membrane proteins. It is conceivable that the eukaryotic ribosome possesses a comparable crevice, as a similar feature could

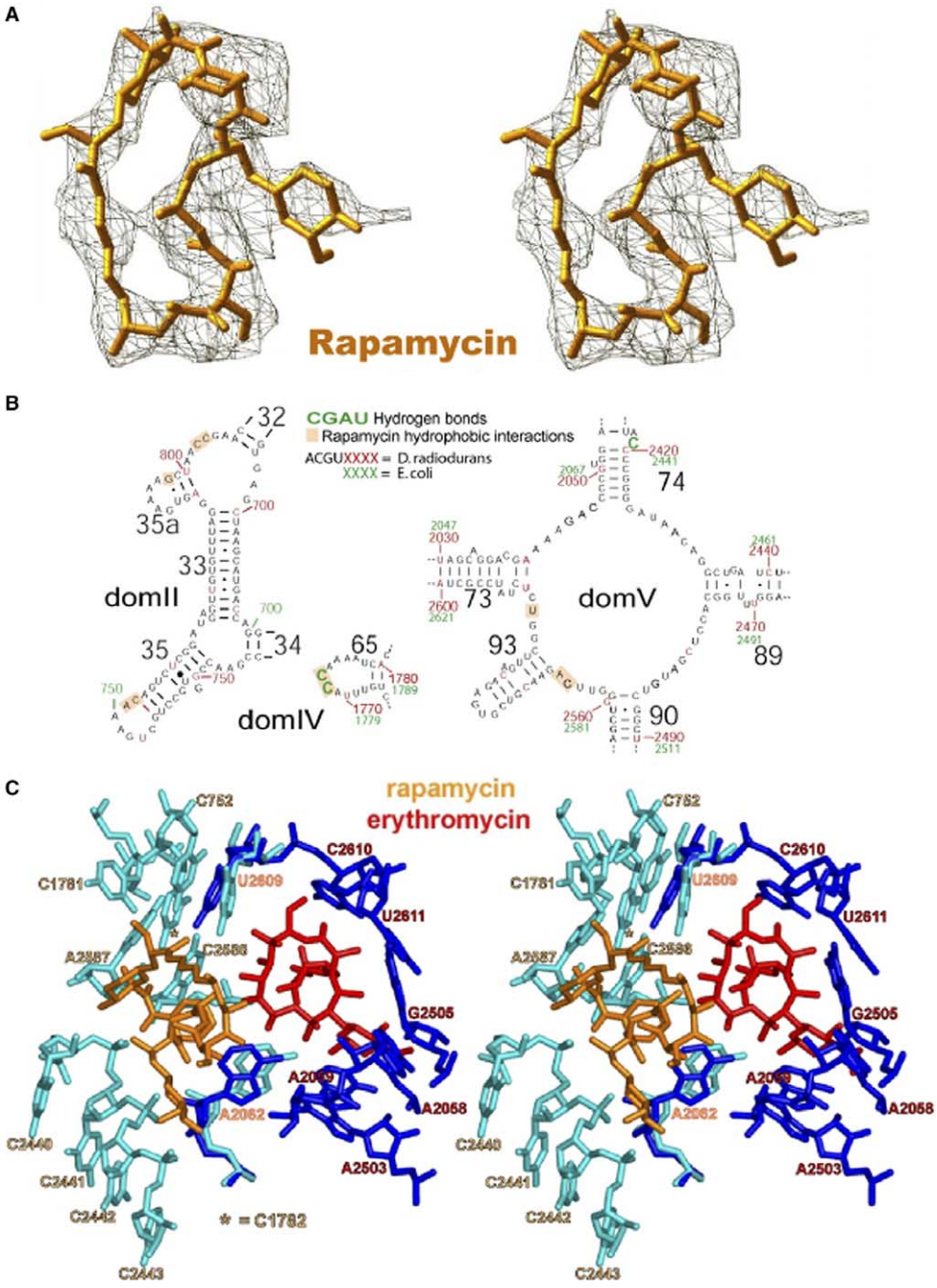

Fig. 2. (A) A stereo view of rapamycin omit ($F_o - F_c$) electron-density-map. (B) The two-dimensional representation of the 23S rRNA nucleotides involved in macrolide binding. Translation code from *E. coli* to *D. radiodurans* is also shown. (C) A stereo view of 23S RNA nucleotides interacting with rapamycin (cyan). For comparison, the 23S RNA nucleotides interacting with erythromycin are shown in blue. Note the differences in the conformations of nucleotides A2602 and U2609, induced by rapamycin binding.

be identified also in the archaeal H50S. However, although we postulate the existence of a crevice in ribosomes from all kingdoms of life, we do not imply structural identity. Thus, phylogenetic diversity should play a considerable role in its detailed structure, as found at the macrolide-binding pocket [10,20,43]. Hence, the binding affinities of this crevice may vary, explaining why rapamycin is not known to strongly inhibit membrane proteins translation.

The cotranslational folding may be only transient, until messages are transmitted to other cell components (e.g., the translocone pore [7,42]). Alternatively, it is conceivable that once small nucleation centers are formed, they may progress through the tunnel by temporary expansions of the tunnel-diameter, as observed recently for translation-arrested ribosomes [44]. Thus, our provisional assignment of the crevice functional role can be integrated into our previous findings concerning the tunnel dynamic properties that enable its participation in polypeptide elongation and arrest, sequence discrimination and signaling to various cellular components, including the ER membrane.

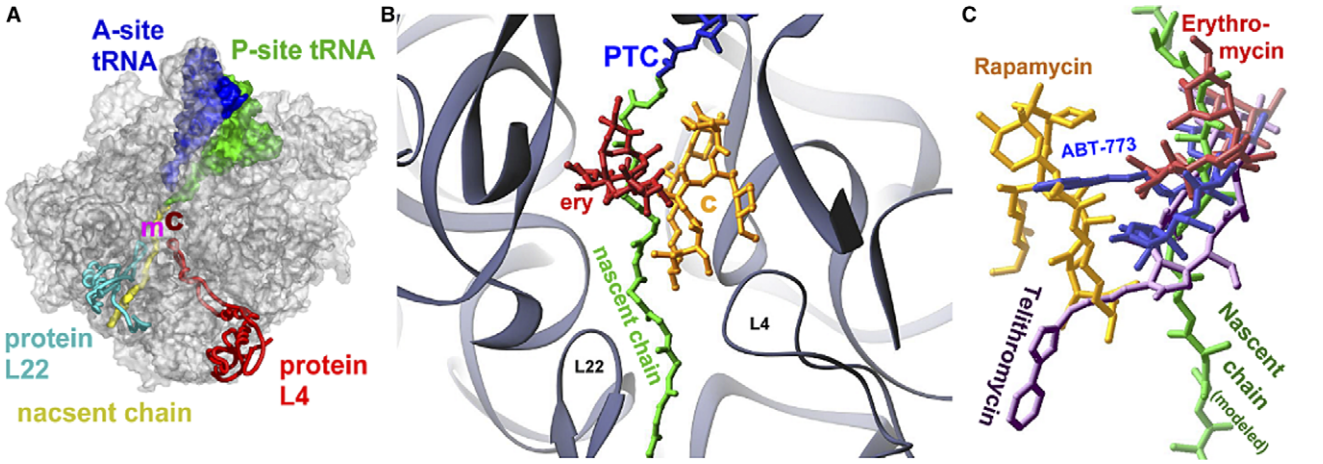

Fig. 3. (A) The positions of rapamycin crevice, C, in relation to the macrolide-binding site, m, and the tunnel constriction composed of the tips of the elongated loops of proteins L4 and L22. The large ribosomal subunit form *D. radiodurans* [2], sectioned so that the internal exit tunnel can be seen, is shown in transparent gray. Also shown are the A- and P-site tRNAs, docked on the large subunit using the structure of the entire ribosome complex [39] and a modeled nascent chain [9]. (B) A more detailed view of the ribosomal components around rapamycin binding site. Erythromycin binding site is also shown, for comparison. (C) Superposition of the locations of rapamycin, erythromycin, telithromycin and ABT-773 in D50S.

However, the finding of the feature that may act as an intra-ribosome chaperon does not provide sufficient structural tools for answering fundamental questions such as: do nascent chains retain a single or acquire multi-conformations while traveling through the tunnel? Is there a signaling mechanism dictating the nascent chain conformation and initiating local folding? Does the tunnel normally switch between open and constricted conformations? What is the conformational state of nascent chains when they emerge out of the exit tunnel?

3.2.1. Medical implications. The binding mode observed for rapamycin suggested that anchoring to the tunnel is only a prerequisite for the polyketide antibiotic function. Indeed, rapamycin binding crevice is located aside the typical macrolide-binding pocket (Figs. 1C and 3B and C). Furthermore, by modeling a nascent chain in the exit tunnel, we show that, different from macrolides and ketolides studied so far, rapamycin-binding mode leaves sufficient tunnel space for the nascent chain (Fig. 3B and C). Our present results are therefore consistent with previous observations that a necessary requirement for efficient antibiotic activity of macrolide-like compounds is their binding to the ribosome exit tunnel, in a manner that efficiently blocks the tunnel. So far, we found that this mode of binding is conferred to macrolides and ketolides by their desosamine sugars [9,16–18]. Rapamycin binding to eubacterial ribosomes may be exploited for designing improved antibiotics.

A2058 is the primary macrolide-binding nucleotide, via its desosamine sugar [18] and is implicated in macrolide resistance and selectivity via mechanisms based on modifications of its base, either by di-methylation by Erm methylases or by mutation to guanine, the nucleotide commonly found at this position in eukaryotes and archaea [40]. Since rapamycin binding does not involve the nucleotide at position 2058, it appears that erythromycin and MLS resistance-inducing mutations would not affect rapamycin binding. Furthermore, as the desosamine sugar of macrolides and ketolides plays an important role in their binding, the study of the binding interactions of a molecule resembling macrolides, albeit lacking a desosamine sugar, should lead to the identification of novel binding patches of the ribosome exit tunnel for which no resistance has yet been developed by bacterial strains.

Rapamycin central ring is significantly larger than those of macrolides, which consist typically of 14–16 atoms. It was found that the flexibility of this ring increases as a function of its size, resulting in the binding of macrolides with 15 or 16-memebered rings to ribosomes having G in position 2058, such as H50S, which do not bind typical macrolides at all [45]. Similarly, it is likely that the increased flexibility of rapamycin central ring could be used for designing new antibiotics. Finally, despite the partial overlap between rapamycin and the macrolide and ketolide binding sites, no cross-reactivity was observed between these compounds (M. Amit, unpublished data). Hence, a careful comparison between the effective and non-effective modes of binding, namely between the telithromycin, ABT-773 (cethromycin) and rapamycin, can identify the minimal requirements for therapeutic effectiveness.

4. Conclusions

Analysis of the crystal structure of D50S in complex with rapamycin showed that rapamycin binds to the ribosome exit tunnel in a crevice located aside the typical macrolide-binding pocket. Our structural results constitute the first example of a non-inactivating binding to the ribosome, thus suggesting that binding to the tunnel is not sufficient to guarantee biosynthesis inactivation. Thus, we identified a crevice at the walls of the exit tunnel that may play a functional role in cotranslational folding and ribosome-cell signaling, as a non-ribosomal compound binds to it in a specific way.

Acknowledgements: We thank Gad Glaser for his guidance in footprinting, to all members of the ribosomes groups in Rehovot, Hamburg and Berlin for participating in this work, especially Frank Schluenzen for his contribution to map interpretation, Paola Fucini and Daniel Wilson for showing that rapamycin does not inhibit protein biosynthesis and does not compete with erythromycin. Data were collected with the help, guidance and assistance of the staff at ID19/

SBC/APS and ID29/ESRF/EMBL. Funds were provided by Regione Campania, L.R. N.5-2002 (R.B.), the US-National-Institute-of-Health (GM34360), the Max-Planck Society, the Human Frontier Science Program Organization (HFSP: RGP0076/2003), and the Kimmelman Center for Macromolecular Assembly. A.Y. holds the Helen and Martin S. Kimmel Professorial Chair.

References

[1] Ban, N., Nissen, P., Hansen, J., Moore, P.B. and Steitz, T.A. (2000) The complete atomic structure of the large ribosomal subunit at 2.4 Å resolution. Science 289, 905–920.
[2] Harms, J., Schluenzen, F., Zarivach, R., Bashan, A., Gat, S., Agmon, I., Bartels, H., Franceschi, F. and Yonath, A. (2001) High resolution structure of the large ribosomal subunit from a mesophilic eubacterium. Cell 107, 679–688.
[3] Walter, P. and Johnson, A.E. (1994) Signal sequence recognition and protein targeting to the endoplasmic reticulum membrane. Annu. Rev. Cell Biol. 10, 87–119.
[4] Stroud, R.M. and Walter, P. (1999) Signal sequence recognition and protein targeting. Curr. Opin. Struct. Biol. 9, 754–759.
[5] Tenson, T. and Ehrenberg, M. (2002) Regulatory nascent peptides in the ribosomal tunnel. Cell 108, 591–594.
[6] White, S.H. and von Heijne, G. (2004) The machinery of membrane protein assembly. Curr. Opin. Struct. Biol. 14, 397–404.
[7] Etchells, S.A. and Hartl, F.U. (2004) The dynamic tunnel. Nat. Struct. Mol. Biol. 11, 391–392.
[8] Johnson, A.E. (2005) The co-translational folding and interactions of nascent protein chains: a new approach using fluorescence resonance energy transfer. FEBS Lett. 579, 916–920.
[9] Berisio, R., Schluenzen, F., Harms, J., Bashan, A., Auerbach, T., Baram, D. and Yonath, A. (2003) Structural insight into the role of the ribosomal tunnel in cellular regulation. Nat. Struct. Biol. 10, 366–370.
[10] Baram, D. and Yonath, A. (2005) From peptide-bond formation to cotranslational folding: dynamic, regulatory and evolutionary aspects. FEBS Lett. 579, 948–954.
[11] Nakatogawa, H. and Ito, K. (2002) The ribosomal exit tunnel functions as a discriminating gate. Cell 108, 629–636.
[12] Gong, F. and Yanofsky, C. (2002) Instruction of translating ribosome by nascent peptide. Science 297, 1864–1867.
[13] Bashan, A., Agmon, I., Zarivach, R., Schluenzen, F., Harms, J., Berisio, R., Bartels, H., Franceschi, F., Auerbach, T., Hansen, H.A.S., Kossoy, E., Kessler, M. and Yonath, A. (2003) Structural basis of the ribosomal machinery for peptide bond formation, translocation, and nascent chain progression. Mol. Cell 11, 91–102.
[14] Bashan, A., Zarivach, R., Schluenzen, F., Agmon, I., Harms, J., Auerbach, T., Baram, D., Berisio, R., Bartels, H., Hansen, H.A., Fucini, P., Wilson, D., Peretz, M., Kessler, M. and Yonath, A. (2003) Ribosomal crystallography: peptide bond formation and its inhibition. Biopolymers 70, 19–41.
[15] Agmon, I., Auerbach, T., Baram, D., Bartels, H., Bashan, A., Berisio, R., Fucini, P., Hansen, H.A., Harms, J., Kessler, M., Peretz, M., Schluenzen, F., Yonath, A. and Zarivach, R. (2003) On peptide bond formation, translocation, nascent protein progression and the regulatory properties of ribosomes. Eur. J. Biochem. 270, 2543–2556.
[16] Berisio, R., Harms, J., Schluenzen, F., Zarivach, R., Hansen, H.A., Fucini, P. and Yonath, A. (2003) Structural insight into the antibiotic action of telithromycin against resistant mutants. J. Bacteriol. 185, 4276–4279.
[17] Schluenzen, F., Harms, J.M., Franceschi, F., Hansen, H.A., Bartels, H., Zarivach, R. and Yonath, A. (2003) Structural basis for the antibiotic activity of ketolides and azalides. Structure 11, 329–338.
[18] Schluenzen, F., Zarivach, R., Harms, J., Bashan, A., Tocilj, A., Albrecht, R., Yonath, A. and Franceschi, F. (2001) Structural basis for the interaction of antibiotics with the peptidyl transferase centre in eubacteria. Nature 413, 814–821.
[19] Harms, J., Schluenzen, F., Fucini, P., Bartels, H. and Yonath, A. (2004) Alterations at the peptidyl transferase centre of the ribosome induced by the synergistic action of the streptogramins dalfopristin and quinupristin. BMC Biol. 2 (4), 1–10.
[20] Auerbach, T., Bashan, A. and Yonath, A. (2004) Ribosomal antibiotics: structural basis for resistance, synergism and selectivity. Trends Biotechnol. 22, 570–576.
[21] Wittmann, H.G., Stoffler, G., Apirion, D., Rosen, L., Tanaka, K., Tamaki, M., Takata, R., Dekio, S. and Otaka, E. (1973) Biochemical and genetic studies on two different types of erythromycin resistant mutants of *Escherichia coli* with altered ribosomal proteins. Mol. Gen. Genet. 127, 175–189.
[22] Davydova, N., Streltsov, V., Wilce, M., Liljas, A. and Garber, M. (2002) L22 ribosomal protein and effect of its mutation on ribosome resistance to erythromycin. J. Mol. Biol. 322, 635–644.
[23] Gabashvili, I.S., Gregory, S.T., Valle, M., Grassucci, R., Worbs, M., Wahl, M.C., Dahlberg, A.E. and Frank, J. (2001) The polypeptide tunnel system in the ribosome and its gating in erythromycin resistance mutants of L4 and L22. Mol. Cell 8, 181–188.
[24] Ranganathan, A., Timoney, M., Bycroft, M., Cortes, J., Thomas, I.P., Wilkinson, B., Kellenberger, L., Hanefeld, U., Galloway, I.S., Staunton, J. and Leadlay, P.F. (1999) Knowledge-based design of bimodular and trimodular polyketide synthases based on domain and module swaps: a route to simple statin analogues. Chem. Biol. 6, 731–741.
[25] Rowe, C.J., Bohm, I.U., Thomas, I.P., Wilkinson, B., Rudd, B.A., Foster, G., Blackaby, A.P., Sidebottom, P.J., Roddis, Y., Buss, A.D., Staunton, J. and Leadlay, P.F. (2001) Engineering a polyketide with a longer chain by insertion of an extra module into the erythromycin-producing polyketide synthase. Chem. Biol. 8, 475–485.
[26] Raught, B., Gingras, A.C. and Sonenberg, N. (2001) The target of rapamycin (TOR) proteins. Proc. Natl. Acad. Sci. USA 98, 7037–7044.
[27] Powers, T. and Walter, P. (1999) Regulation of ribosome biogenesis by the rapamycin-sensitive TOR-signaling pathway in *Saccharomyces cerevisiae*. Mol. Biol. Cell 10, 987–1000.
[28] Zaragoza, D., Ghavidel, A., Heitman, J. and Schultz, M.C. (1998) Rapamycin induces the G0 program of transcriptional repression in yeast by interfering with the TOR signaling pathway. Mol. Cell. Biol. 18, 4463–4470.
[29] Martin, D.E., Soulard, A. and Hall, M.N. (2004) TOR regulates ribosomal protein gene expression via PKA and the Forkhead transcription factor FHL1. Cell 119, 969–979.
[30] Preiss, T., Baron-Benhamou, J., Ansorge, W. and Hentze, M.W. (2003) Homodirectional changes in transcriptome composition and mRNA translation induced by rapamycin and heat shock. Nat. Struct. Biol. 10, 1039–1047.
[31] Dennis, P.B., Jaeschke, A., Saitoh, M., Fowler, B., Kozma, S.C. and Thomas, G. (2001) Mammalian TOR: a homeostatic ATP sensor. Science 294, 1102–1105.
[32] Kim, W.S., Xu, L., Souw, D., Fang, A. and Demain, A.L. (2002) An unexpected inhibitory effect of rapamycin against germination of spores of Bacillus brevis strain Nagano. J. Antibiot. 55, 650–654.
[33] Otwinowski, Z. and Minor, W. (1997) Processing of X-ray diffraction data collected in oscillation mode in: Methods in Enzymology (Carter, C.W. Jr.Jr. and Sweet, R.M., Eds.), Macromolecular Crystallography, Part A, Vol. 276, pp. 307–326, Academic Press, London.
[34] Brunger, A.T., Adams, P.D., Clore, G.M., DeLano, W.L., Gros, P., Grosse-Kunstleve, R.W., Jiang, J.S., Kuszewski, J., Nilges, M., Pannu, N.S., Read, R.J., Rice, L.M., Simonson, T. and Warren, G.L. (1998) Crystallography and NMR system: a new software suite for macromolecular structure determination. Acta Crystallogr. D 54, 905–921.
[35] Jones, T.A., Zou, J.Y., Cowan, S.W. and Kjeldgaard (1991) Improved methods for building protein models in electron density maps and the location of errors in these models. Acta Crystallogr. A 47, 110–119.
[36] Bailey, S. (1994) The CCP4 suite – programs for protein crystallography. Acta Crystallogr. D 50, 760–763.
[37] Carson, M. (1997) Ribbons (Sweet, R.M. and Carter, C.W., Eds.), Methods in Enzymology, Macromol. Crystallogr. B, Vol. 277, pp. 493–505, Academic Press, New York.

[38] Merryman, C. and Noller, H.F. (1998) Footprinting and modification-interference analysis of binding sites on RNA in: RNA:Protein Interactions (Smith, C.W.J., Ed.), pp. 237–253, Oxford University Press, UK, Oxford.
[39] Yusupov, M.M., Yusupova, G.Z., Baucom, A., Lieberman, K., Earnest, T.N., Cate, J.H. and Noller, H.F. (2001) Crystal structure of the ribosome at 5.5 Å resolution. Science 292, 883–896.
[40] Weisblum, B. (1995) Erythromycin resistance by ribosome modification. Antimicrob. Agents Chemother. 39, 577–585.
[41] Douthwaite, S. and Champney, W.S. (2001) Structures of ketolides and macrolides determine their mode of interaction with the ribosomal target site. J. Antimicrob. Chemother. 48, 1–8.
[42] Woolhead, C.A., McCormick, P.J. and Johnson, A.E. (2004) Nascent membrane and secretory proteins differ in FRET-detected folding far inside the ribosome and in their exposure to ribosomal proteins. Cell 116, 725–736.
[43] Pfister, P., Corti, N., Hobbie, S., Bruell, C., Zarivach, R., Yonath, A. and Bottger, E.C. (2005). 23S rRNA base-pair 2057–2611 determines ketolide susceptibility and fitness cost of the macrolide resistance mutation 2058A → G. Proc. Natl. Acad. Sci. USA (in press).
[44] Gilbert, R.J., Fucini, P., Connell, S., Fuller, S.D., Nierhaus, K.H., Robinson, C.V., Dobson, C.M. and Stuart, D.I. (2004) Three-dimensional structures of translating ribosomes by Cryo-EM. Mol. Cell 14, 57–66.
[45] Hansen, J.L., Ippolito, J.A., Ban, N., Nissen, P., Moore, P.B. and Steitz, T.A. (2002) The structures of four macrolide antibiotics bound to the large ribosomal subunit. Mol. Cell 10, 117–128.